Build Simul (2021) 14: 1511–1523
https://doi.org/10.1007/s12273-020-0757-4

Gaseous pollutant transport from an underground parking garage in a Mediterranean multi-story building—Effect of temporal resolution under varying weather conditions

Rivka Reichman, Yael Dubowski (✉)

Faculty of Civil and Environmental Engineering, Technion – Israel Institute of Technology, Haifa, 32000, Israel

Abstract

Indoor air dynamics and quality in high density residential buildings can be complex as it is affected by both building parameters, pollution sources, and outdoor meteorological conditions. The present study used CONTAM simulations to investigate the intra-building transport and concentration of an inert pollutant continuously emitted from an underground garage of a 15-floor building under moderate Mediterranean weather. The effects of outdoor meteorological conditions (air temperature, wind speed and direction) on indoor distribution of the emitted pollutant was tested under constant conditions. The importance of using actual transient meteorological data and the impact of their temporal resolution on calculated concentrations and exposure levels were also investigated. Vertical profiles of air exchange rate (AER) and CO concentration were shown to be sensitive to indoor–outdoor temperature difference, which controls the extent of the stack effect and its importance relative to wind effect. Even under constant conditions, transient mode simulations revealed that the time needed for pollutant distribution to reach steady state can be quite long (>24h in some cases). The temporal resolution (1h vs. 8h) of the meteorological data input was also found to impact calculated exposure levels, in an extent that varied with time, meteorological conditions and apartment position.

Keywords

CONTAM;
indoor air quality;
high rise residential buildings;
stack effect;
wind effect;
inter-flat dispersion;
variable meteorological data effect

Article History

Received: 14 May 2020
Revised: 29 November 2020
Accepted: 10 December 2020

1 Introduction

In modern society the majority of people spend most of their time (>80%) indoors, and therefore indoor air quality (IAQ) is likely to have a strong impact on their health (Robinson and Nelson 1995; Klepeis et al. 2001; Sundell 2004). Moreover, people who are exposed to indoor air pollutants for long periods of time are often those most vulnerable to pollution effects (chronically sick people, elderly and infants). Due to increasing urbanization and population growth, high rise residential (HRR) buildings are becoming more abundant (UNFPA 2007).

Pollutant transport in buildings is controlled by airflows that are driven by pressure difference caused by stack effect, wind effect and mechanical ventilation systems. Stack effect occurs when there is an indoor–outdoor temperature difference (ΔT). When wind impinges on a building it creates pressure on the building envelope that can be calculated using Bernoulli's equation. The resulting time-averaged surface pressure is given by (ASHRAE 2013):

$$P_w = C_p \rho_o v^2 / 2 \quad (1)$$

where, P_w – wind pressure (Pa), ρ_o – outdoor air density (kg/m^3), v – wind speed at building height (m/s), and C_p – pressure coefficient.

Wind flow patterns around buildings are characterized by turbulence and are strongly affected by building geometry and local shielding. Equation (1) accounts for these effects by using the wind pressure coefficient (WPC), C_p. Wind pressures are generally positive with respect to the undisturbed airstream on the windward side of a building and negative on the leeward sides. When both stack and wind effects exist, the pressures caused by each are added together to determine the total pressure difference across the building envelope.

E-mail: yaeld@technion.ac.il

Previous studies on pollutant transport in HRR buildings include on-site measurements of pressure difference (Jo et al. 2007; Lim et al. 2011) and trace gas transmission (Wu et al. 2016; Song et al. 2019) in addition to numerical simulation of airflows (Jo et al. 2007; Lim et al. 2010, 2011; Mao et al. 2015; Yang and Gao 2015), pollutant dispersion (Lim et al. 2010, 2011; Mao et al. 2015; Yang and Gao 2015), and wind tunnel studies (Mu et al. 2016, 2017). Since stack effect is of considerable importance during cold winter season, studies related to stack effect (Lim et al. 2010, 2011; Yang and Gao 2015) and the combined stack and wind effect (Mao et al. 2015) were carried out under noticeable positive ΔT (i.e., $\Delta T \geq 5$ °C). The studies related to the wind effect on cross-contamination between apartments within the same building (Mu et al. 2016, 2017; Wu et al. 2016) were performed under slightly positive ΔT (≈ 0.5 °C). Most of these studies were performed under constant weather conditions with a prime concern to spatial dispersion. Yang and Gao (2015) and Mao et al. (2015) studied the temporal dispersion under constant weather condition as well. Results indicate that pollutants may travel vertically and horizontally in buildings depending on weather conditions (i.e., ΔT and wind pattern) and on source location. Clearly, opening windows/doors will also affect air and pollutant dynamics indoors, but for practicality transport simulations in multi-story buildings commonly assume closed windows (i.e., air exchange with outdoor atmosphere occur solely through cranks (Jo et al. 2007; Lim et al. 2010, 2011; Mao et al. 2015; Yang and Gao 2015). Airflow and indoor gaseous pollutant transport through window openings are usually simulated for small scale scenario (i.e., two rooms) using computational fluid dynamics (CFD) (Mao and Gao 2015; Liang and Qin 2017).

While previous studies provided essential information on air dynamics and pollutant transport in HRR buildings, most of them were carried out under constant weather conditions with positive ΔT (i.e., $T_{indoor} > T_{outdoor}$), which is not the case for many large cities located at low-latitudes and warm regions. To the best of our knowledge, Li et al. (2005) is the only numerical study that used variable weather conditions measured during two peak days of the SARS outbreak in Amoy Garden. However, in the study variable weather data were only used to explore the routes of spatial dispersion with no further investigation of the effect of the transient conditions and their temporal resolution on spatial and temporal transmission of pollutant inside the HRR building.

Meteorological parameters have a characteristic diurnal pattern that can affect the transport of pollutants from underground garages to different parts of the building due to their influence on the forces driving the pollutant transport; stack and wind effects. Stack effect is the main driving force for the vertical transport (Mao et al. 2015; Yang and Gao 2015) and is depended on ΔT. Under conditions where $T_{out} < T_{in}$, airflow direction is upward and stack effect magnitude increases as ΔT increases. Thus, for continuous emissions, the highest concentrations in the upper floors are expected at nighttime when ΔT is the highest (Mao et al. 2015; Yang and Gao 2015; Song et al. 2019). Wind flow around a building imposes pressure on the building facades that increases as the wind speed (WS) increases, and its sign (positive or negative) depends on the relative direction of the building facade to the wind direction (WD); positive values for windward facade and negative values for the other facades. Pollutant entrance into apartments from shafts and corridors is prevented in the presence of positive pressure in the apartment. Such conditions are more likely to exist in windward side apartments. As a result, the potential of pollutant entrance from shafts and the corridor into apartments is higher on the leeward side of the building. On the course of the diurnal cycle, apartments that are in the windward side or leeward side may constantly change.

In the present study CONTAM simulation is applied to study air dynamic and pollutant dispersion in a multi-story building under different temporal resolutions of variable weather conditions typical to Mediterranean climate.

2 Methods

2.1 Overview

Simulations were carried out using CONTAM 3.2, a multi-zone airflow and contaminant transport analysis software package (Dols and Polidoro 2015). Airflow and contaminant dispersion within the building were predicted based on zone leakage data, weather data and WPCs for all building openings. A detailed description of the governing equations for CONTAM can be found in (Walton 1989) and (Dols and Polidoro 2015). A brief description is given in Section 2.4.

WPC for all the openings were calculated using a CFD approach, for ten configurations of WD striking the building: covering full circle in 30° steps. Settings described in Section 2.3 were used for each configuration to create the geometry and grid as well as to perform the computations.

2.2 Case study description

The building selected as a case study (Figure 1) is a typical residential multi-story building in an urban area on the Israeli coastal plan (32.1°N, 34.8°E). The building is an H-type floorplan building with a center core, an underground parking garage, first-floor lobby, and additional 15 residential floors above it. At the center core there are two elevator shafts and a stairwell shaft connecting all floors. The Lobby

floor (Figure 2(a)) consists of one apartment (Apt. L, 110 m^2), lobby space (164 m^2), a bicycle storage room (44 m^2) and a residence club (88 m^2). Residential floors (1–15) consist of four identical apartments (Apts. A to D, 100 m^2 each) connected to the central core via corridor (Figure 2(b)). All apartments include four rooms (9 to 42 m^2 each), two bathrooms (5–6 m^2) and a utility room (7 m^2). Following the Israeli energy rating of residential buildings (ISI 2017), windows in each apartment have a total area equal to 20% of the apartment area (i.e., 20 m^2). Window area and perimeter range 0.25 to 10 m^2 and 2 to 13 m, respectively. Each floor height was 3 m. The horizontal cross-sectional areas of the corridor, elevator shaft and stairwell shaft were about 20, 8 and 15 m^2, respectively. The entrance to the parking garage is through a 10 m^2 opening. The building structure is made of steel reinforced concrete. For the simulations carried out using CONTAM (detailed below), real architectural plans of the selected building were simplified to present zones and airflows passes (Figure 2). Each residential room was assumed to be an individual zone, as was the corridor, stairwell, and elevator shaft on each floor. The shafts at the center core, which may influence the airflow inside the building, are connected vertically to each other using the CONTAM stairwell and shaft airflow element models. Following previous studies (Jo et al. 2007; Lim et al. 2011) the elevator carriages in the present study were assumed to be static. In additional, all doors and windows were assumed to be kept closed, allowing air flow through their unsealed frames. As mentioned above, although the latter is an oversimplification of reality, it is common practice when simulating air dynamics in multistory buildings.

Air leakage data for all components of the building were taken from published data (Jo et al. 2007; ASHRAE 2013) and are listed in Table 1. Leakage from the garage

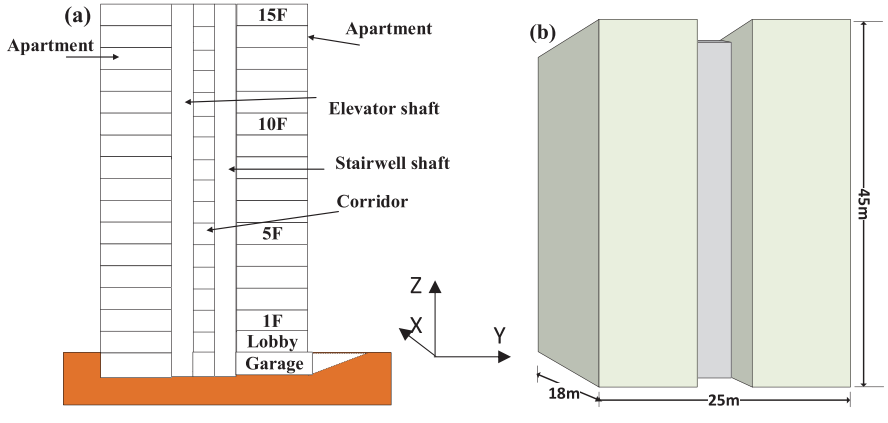

Fig. 1 Schematic outlook of test case building

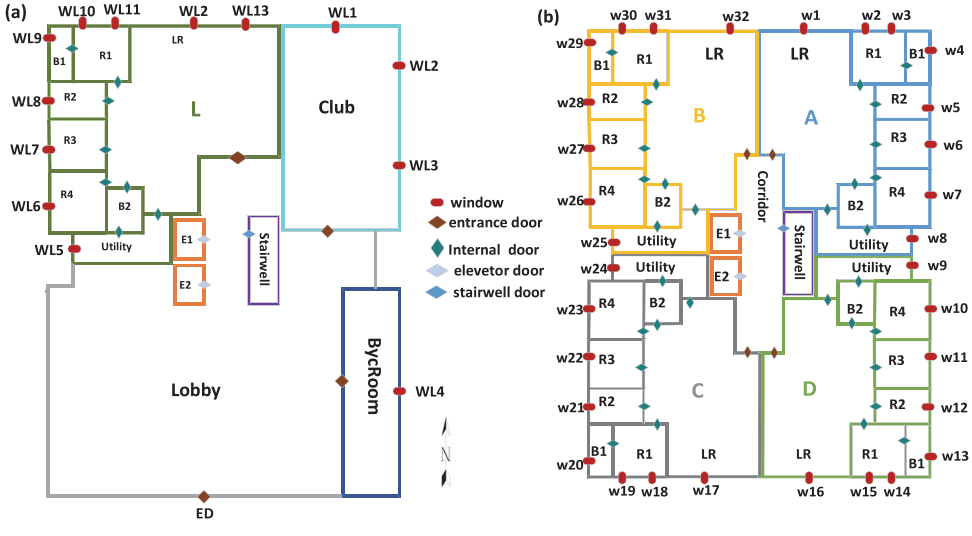

Fig. 2 Top view scheme of (a) lobby floor and (b) residential floors. R – bedroom, B – bathroom, LR – living room, W – window, E – elevator shaft, ED – main entrance door. Locations of doors, which act as main airflow connectors between intrabuilding zones in each floor, are marked by solid diamond symbols. Air exchange with external atmosphere was enabled via windows, which are marked with red ellipses

Table 1 Leakage data used in the multi-zone simulation

Building component	Air leakage data	Reference
External wall, ceiling	0.7 cm^2/m^2 (75 Pa)	ASHRAE 2013
Windows	2.06 cm^2/m (10 Pa)	ASHRAE 2013
Stairwell door	120 cm^2/each (10 Pa)	Jo et al. 2007
Elevator door	325 cm^2/each (10 Pa)	Jo et al. 2007
Flat entrance door	70 cm^2/each (10 Pa)	Jo et al. 2007
Flat internal door	21 cm^2/each (10 Pa)	Jo et al. 2007

ceiling was assumed to be zero.

Carbon monoxide (CO) was selected as the tracer gas to simulate gaseous transport in this residential multi-story building from a source located in its underground parking garage. CO emissions were not considered as a point source since they are generated by several cars occupying the whole garage space, which allows considering the garage as a single zone. A constant CO generation rate of 1.5×10^{-6} kg/s was assumed, based on rates previously reported for underground automobile parking garages (Papakonstantinou et al. 2003; Eshack et al. 2015). The simulation described below was run assuming continuous emissions at the underground garage.

2.3 Wind pressure coefficients (WPC)

2.3.1 CFD model for calculating WPC

The commercial software ANSYS workbench 19.0 was used to calculate WPC over all external openings (Figure 2), assuming that all housing blocks are sealed.

The geometry of the computational model was built in DesignModeler under ANSYS 19.0 according to the shape of the selected building, whose dimensions are 18 m × 25 m × 48 m ($L \times W \times H$; Figure 1(b)). The building was placed in a computational domain (Figure 3), which was large enough (i.e., 500 m × 300 m × 240 m, $L \times W \times H$) to minimize computational artifacts (i.e., block ratio of 1.6%, fulfilling the recommendation to be less than 3% (Tominaga et al. 2008)). The distances between the building walls and the domain's inlet, outlet and roof were 192 m (= 4*H*), 288 m (= 6*H*) and 192 m (= 4*H*), respectively. Calculation-Mesh was generated using the automatic method based on face sizing, curvature size function and high smoothing. All other settings were left on default. An advanced wall function was used for near-wall treatment. Element size on the building surface was 0.005 m, and 305743 elements with 57620 nodes were used. The inlet wind velocity profile in the *x* direction of the domain followed a power law equation (Eq. (2)), while the velocity components in the other directions of the domain (i.e., *y* and *z* directions) were set as zero.

$$U_z = U_{\text{met}}\left(\frac{\delta_{\text{met}}}{H_{\text{met}}}\right)^{\alpha_{\text{met}}}\left(\frac{Z}{\delta}\right)^{\alpha} \tag{2}$$

where, U_{met} = 10 m/s, H_{met} = 10 m, δ_{met} = 0.14, α_{met} = 270 m (i.e., refer to meteorological station at open terrain (ASHRAE 2013), δ = 0.22, and α = 370 m (i.e., refer to urban and suburban areas (ASHRAE 2013).

Fluent 19.0 was used to solve the 3D Reynolds Averaged Navier Stokes (RANS) equations and the continuity equation, using the finite volume method. The RNG *k-ε* model was used to simulate the turbulent effect, and the SIMPLE algorithm was used for pressure velocity coupling. Pressure interpolation was a second order equation. First order upwind discretization schemes were used for both convection terms and viscus terms. Near wall treatment was done near the domain bottom as well as around the building walls periphery. The mesh near the wall was refined using Y^+ adaptation process (Eq. (3)) with the condition $3 < Y^+ < 30$.

$$Y^+ \equiv \frac{\rho u_\tau y}{\mu} \tag{3}$$

where, ρ – air density, μ – molecular air viscosity, y – distance from wall, u_τ – the friction velocity defined as $\sqrt{\frac{\tau_w}{\rho}}$, with τ_w being wall-shear stress (Fluent 2013).

2.3.2 Calculated WPC

WPC distribution for apartments A and B along the various floors under western wind direction (270°) are presented in Figure 4. WPCs on the windward side of the building (i.e., west side windows: W25–W29) have positive values while

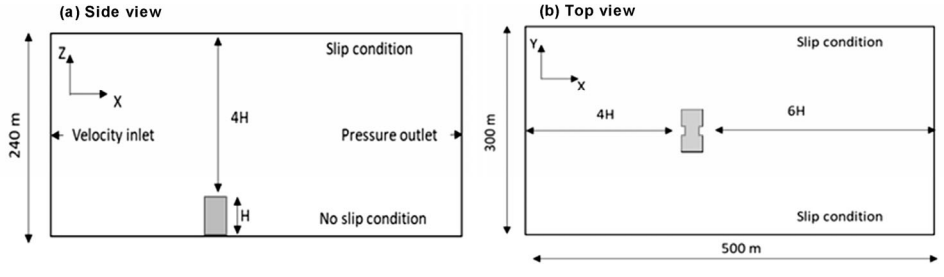

Fig. 3 Schematic description of the CFD model computation domain. *H* represents building height

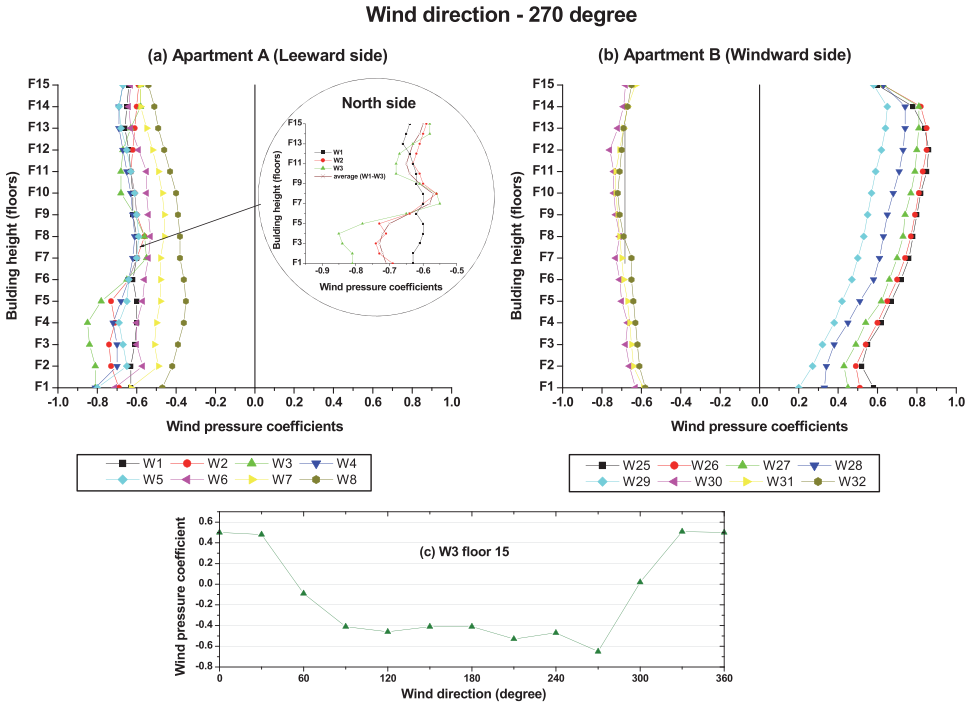

Fig. 4 Predicted WPC along building floors for western WD (270°) on the external windows of (a) apartment A (east (W4–W8) and north (W1–W3) sides), and (b) apartment B (west (W25–W29) and north (W30–W32) sides. The insert in plot (a) shows a zoom-in on the north side windows. (c) Calculated WPC for W3 in the15th floor under various WD (in steps of 30° over 0–360° range)

on all the other sides, including the roof, WPC values are negative. Furthermore, changes in WPC along the building height were larger on windows facing the windward side (i.e., positive WPC values). This behavior can be attributed to the atmospheric pressure profile effects, the general airflow pattern around a bluff body (ASHRAE 2013), and the unique geometrical characteristics of the building shape.

Calculated WPC for WD over the whole 0–360° range, in steps of 30°, were provided to CONTAM as input for each connection to the external atmosphere. Figure 4(c) shows, for example, WPC dependency on WD for W3 at the 15th floor.

2.4 CONTAM – theoretical background

CONTAM is an airflow network model based on mass, chemical species, and energy conservation equations that are solved numerically using the Newton-Raphson method. It models natural ventilation by assigning a node to each zone (e.g., rooms, ambient atmosphere etc.) and flow paths (i.e., airflow elements such as cracks, doors, windows etc.) between them. Conditions within each zone, such as air velocity, temperature, and humidity, are computed based on the pressure difference between zones and their properties. The air within each zone is assumed to be well-mixed with uniform properties. CONTAM provides two simulation modes, steady and transient, to simulate airflow and contaminant transport. In the steady mode user defines steady-state weather data and the output provides a single value for each zone. The transient mode requires a weather file as input and its output consists of a time-series of concentrations for each zone. Modeling varying weather conditions under the transient mode is necessary, and additionally, even under constant weather conditions it enables estimating the response time and indoor concentration buildup rate at the different zones.

Airflow analysis: Flow within each airflow element is controlled by the total pressure drop. The total pressure drop over the building envelope openings is given by:

$$\Delta P = P_i - P_j + P_s + P_w \tag{4}$$

where: P_i and P_j – total pressures at zones i and j, P_s – pressure difference due to density and elevation difference, and P_w – pressure difference due to wind (Eq. (1)).

Equation (4) establishes a sign convention for flow direction, with positive being from zone j to zone i. In the absence of wind ($P_w = 0$) the flow is assumed to be governed by Bernoulli's equation.

Most infiltration models are based on the power law relationship between airflow and pressure difference across a crack or opening in the building envelope (Eq. (5)):

$$Q = C(\Delta P)^n \text{ or } F = C(\Delta P)^n \tag{5}$$

where, Q – volumetric flow rate (m^3/s), F – mass flow rate (kg/s), ΔP – pressure drop across the opening (Pa), C – flow coefficient, and n – empirical flow exponent.

Theoretically, flow exponent value should lie between 0.5 and 1.0. Large openings are characterized by values very close to 0.5, while values near 0.65 have been found for small crack-like openings. The power law equation can be used with component leakage area formulation (ASHRAE 2013). The great advantage of the latter formulation is the availability of effective leakage area values for a variety of elements from literature (ASHRAE 2013). The power law equation can also be treated as an orifice equation (Dols and Polidoro 2015). This approach is used in CONTAM to calculate airflow in stairwell and elevator shafts as well. The flow coefficient for the stairwell is calculated using relationships based on empirical data (Achakji and Tamura 1988), while the coefficient for the elevator shaft is based on a conduit friction model using the Darcy-Weisbach relation and Colebrook's equation for the friction factor (ASHRAE 2013).

The CONTAM model for airflow in stairwells uses empirical values (Achakji and Tamura 1988). Airflow in the elevator shaft is modeled using the shaft power-law flow element. This airflow element allows the user to enter a description of a shaft, which is then converted by CONTAM to a power-law relationship, assuming a pressure exponent of 0.5. The flow coefficient in this case is based on a conduit friction model using the Darcy-Weisbach relation and Colebrook's equation for the friction factor (ASHRAE 2013).

Contaminant Analysis: For inert contaminants, concentrations are calculated using the following mass balance equation,

$$\frac{dm_i^\alpha}{dt} = \sum_j F_{j\to i}\left(1-\eta_j^\alpha\right)C_j^\alpha + G_i^\alpha - \sum_j F_{i\to j}C_i^\alpha \quad (6)$$

where m_i^α – the mass of contaminant α in control volume i (kg), $F_{j\to i}$ – air mass flow rate from control volume j to control volume i (kg/s), η_j^α – the filter efficiency in the airflow path (0–1), C_j^α – the mass concentration of contaminant α in control volume j (kg/kg), G_i^α – contaminant α generation rate in control volume i (kg/s), $F_{i\to j}$ – air mass flow rate from control volume i to control volume j (kg/s), and C_i^α – the mass concentration of contaminant α in control volume i (kg/kg).

2.5 Simulation procedure

In the first stage of the current research, simulations are run under constant meteorological conditions, examining the effect of wind and ΔT on AER and resulting indoor distribution of emitted pollutant. The second stage of this work applies simulation under more realistic varying meteorological conditions, testing the effect of temporal resolution (TR) of input data on obtained indoor concentrations and resulting exposures.

2.5.1 *Constant weather conditions*

The effect of ΔT, WS and building facade direction relative to WD on air exchange rate (AER) and gaseous pollutant transport within the building are tested under constant weather conditions over 48h using transient simulation method. These simulations enable evaluating the temporal response of pollutant buildup in various building sections.

During simulations, temperatures of the garage, corridors, elevator and stairwell shafts are set constant at 20 °C, while apartment's temperature was 23 °C. Outdoor temperature (T_{out}) is set to 10 °C and 20 °C since these values represent, respectively, average outdoor temperatures in the Israeli coastline during winter (January–February) and transition seasons (fall and spring) (IMS Israel Meteorological Service 2020). WD is set constant as 270° (westerly wind). Under these conditions apartments A and B are on the leeward and windward sides of the building, respectively. Wind speed values of 0, 2, 4 and 6 m/s are used for the weather conditions effect on AER, and the value of 4 m/s is used for the effect on pollutant transport.

2.5.2 *Varying weather condition*

To better represent real-life scenarios, transient mode simulations are conducted using meteorological data (MD) measured at the Tel-Aviv coast meteorological station during 15–18 January 2017 (IMS Israel Meteorological Service 2020). WD is averaged using the vector averaging method. Temperatures inside the building are kept as described in constant weather simulations.

The effect of temporal resolution of MD on calculated concentrations is examined for all four apartments over 8h emission time, using 1h and 8h averaged MD as input, during daytime (8:00–16:00) and night hours (22:00–6:00). The effect of temporal resolution of MD on the accumulated exposure is tested over 72h period.

3 Results and discussion

3.1 The effect of weather parameters under constant weather conditions

3.1.1 *AER*

AER distribution over the examined building is studied for apartments A and B representing, respectively, apartments with leeward and windward walls. Apartments C and D are identical in that regard to apartments B and A, respectively.

The obtained temporal trend of AER indicates that this parameter reaches steady state values very quickly (< 1h). Predicted AER for the two apartments under wind speed (WS) ranging from 0 to 6 m/s and T_{out} of 10 °C and 20 °C are shown in Figure 5.

Under stack effect conditions (i.e., WS = 0), when buoyancy is the only airflow driving force, similar AER values are obtained for both apartments (Figure 5). In the presence of wind, predicted AER on the windward side of the building (apartment B) are higher than those on leeward side (apartment A) at all floors.

Under colder weather conditions, where $T_{out} < T_{in}$, both stack and wind effects should be considered. The absolute values of calculated AER vary between 0.05 and 0.25 h^{-1} for apartment A (leeward) and 0.05 and 0.30 h^{-1} for apartment B (windward), depending on floor height and wind speed. As expected (Yang and Gao 2015), the highest AER is obtained for the top floor (#15) on the windward-side apartment under the highest wind speed (6 m/s). The lowest absolute values are obtained close to Neutral Pressure Level (NPL) location, which depends on ΔT, WS and WD.

Airflow direction (i.e., infiltration or exfiltration) depends on NPL location, with infiltration (positive AER) observed at floors below NPL and exfiltration (negative AER) at floors above it. Under the tested conditions, increasing wind speed results in an elevation of NPL position on windward side and vice versa on leeward side (Figure 5(a)). A similar trend is reported by Mao et al. (2015), who studied AER in a 33-floor building under comparable weather condition.

Under conditions where ΔT is negligible (i.e., T_{out} = 20 °C), AER values are lower than observed under positive ΔT, ranging 0.02–0.15 h^{-1} and 0.02–0.23 h^{-1} for apartments A and B, respectively. Absolute AER values showed strong positive dependency on WS. Under WS > 0, infiltration is observed in the windward apartment (Figure 5(c)) and exfiltration in the leeward side (Figure 5(d)) at all floors. This lack of dependency on floor height is not surprising considering that under conditions where stack effect is negligible (i.e., $T_{out} \approx T_{in}$), AER variation along building floors is expected to be governed by WPC distribution over building height. Indeed, WPC calculated under such conditions (western wind and T_{out} = 20 °C), shows quite uniform vertical profiles (Figure 4).

3.1.2 *CO concentration profile*

Unlike AER, indoor CO concentrations depict a slower temporal response, which depends both on meteorological conditions and location within buildings as discusses below. Overall, under the current conditions ($\Delta T \geq 0$) the airflow caries CO emitted at the underground garage to upper floors through the elevator and stairwell shafts. In each floor, airflow with its CO content may enter the public corridor whenever a negative pressure gradient exists between corridor and shafts (i.e., $P_{corridor} < P_{shaft}$). The airflow loop between this central corridor and the different apartments will follow the pressure gradient that depends on the wind properties.

- *T_{out} = 10 °C (ΔT = 10 °C)*:

Temporal profiles of CO concentration in apartments and building public spaces over 48 hours are depicted in Figure 6.

An increase in CO concentrations at the elevator shaft started on all floors almost immediately after emission

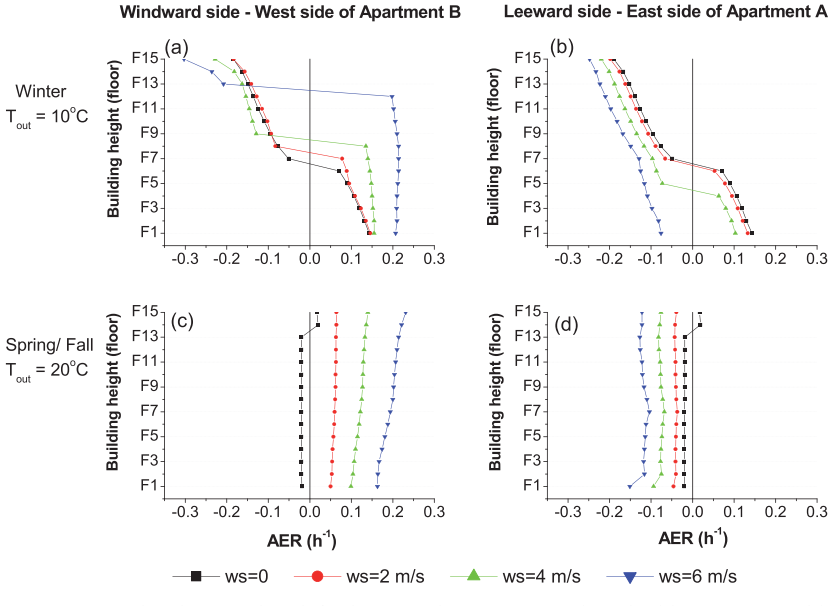

Fig. 5 AER (h^{-1}) for apartments A (right plots) and B (left plots), under positive and negligible ΔT (top and bottom plots, respectively) and different wind speeds. In all cases wind direction is 270° (western wind) and T_{in} = 20 °C

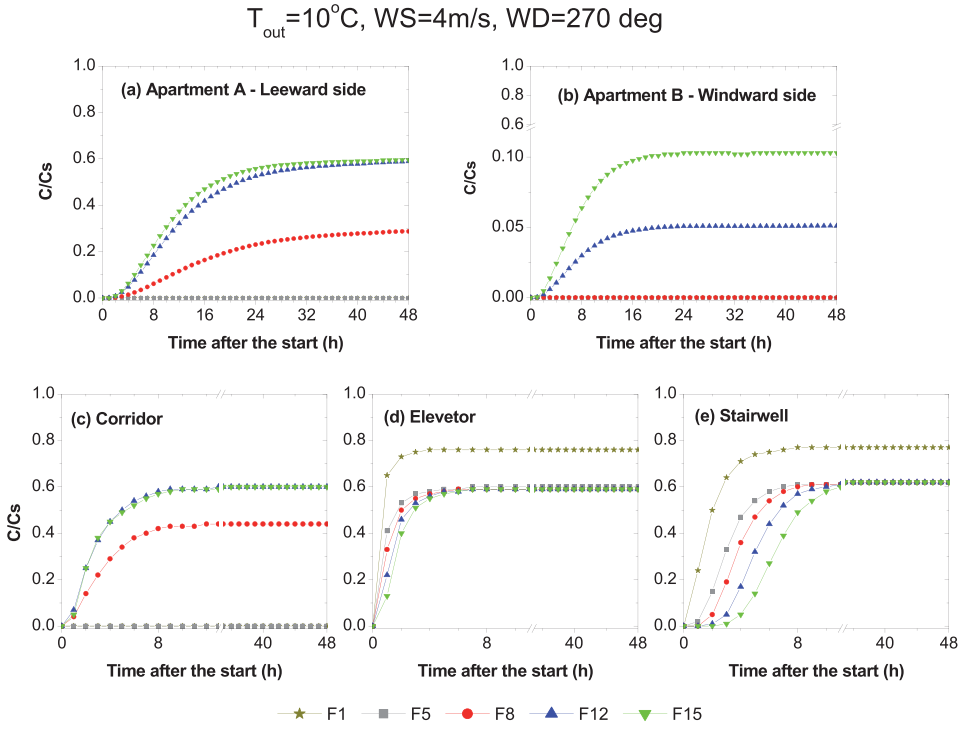

Fig. 6 Variation of normalized concentration over time at selected floors for (a) apartment A, and (b) apartment B, (c) corridor, (d) elevator shaft, and (e) stairwell shaft. Weather conditions: T_{out} = 10 °C, WS = 4 m/s and WD = 270°

started, probably due to its continuous shape connecting all floors. In the stairway shaft pollutant accumulation shows dependency on floor height; with no lag time at the garage and lobby floor and up to a 3h delay at the top 15th floor. In the apartments and corridors above the NPL, concentrations start to increase after 2h, while below the NPL they remain around zero. These results agree well with a previous report by Mao et al. (2015). The highest normalized concentration values for apartments A, B and corridor, are observed at the top floor (0.6, 0.1 and 0.6, respectively), while for both elevator and stairwell shafts the highest steady concentration (0.77) is observed at the 1st floor.

In addition to the differences in lag-time among the different building sections, Figure 6 shows a difference between them in the time needed for reaching steady-state concentration. In line with lag-time observations, the locations that seem to have better vertical mixing appeared to also have the shortest time to reach steady-state concentrations; 8h for elevator shafts at all floors as well as at the stairwell shaft on floors below the NPL and 12h for all floors above it, about 16h for windward apartment B, and maximal built-up time of over 30h at the leeward apartments (Figure 6). Nevertheless, after 8 h concentration profiles for the windward apartment, corridor, elevator, and stairwell shafts became very close to those at steady state (e.g., for apartment B normalized concentration of 0.07 after 8h vs. 0.1 at steady state). On the other hand, for the leeward apartment, even after 12h, the concentration on floors above the NPL are only about half the values received after 48h.

- T_{out} = 20 °C (ΔT ~ 0 °C):

Reducing ΔT to about zero eliminates stack effect and makes wind effect the dominant force effecting intra-building mixing. The resulting more limited vertical transport at ΔT ~ 0 alters the shape of the concentration profiles (Figure 7) and enhances lag- and build-up times for pollutant concentrations (especially at the top floors) in the leeward apartment, corridor, elevator and stairwell shaft, relative to rates observed under ΔT > 0 (Figures 8 vs. 6). Opposite

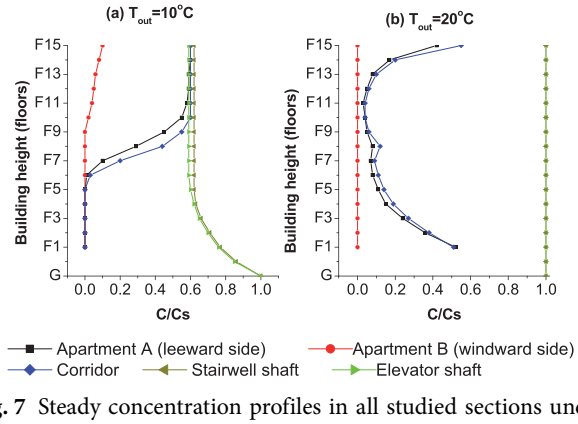

Fig. 7 Steady concentration profiles in all studied sections under (a) positive ΔT and (b) negligible ΔT. WD in all cases is 270° (western wind)

to $\Delta T > 0$ conditions, in the absence of stack effect, the lag-time in concentration build-up increases with height at all tested sections. Lag times at the 1st and 15th floors varied between 2 and 6h for apartment A, 1 and 5h for the corridor, 1 and 5h for the elevator shaft and 1 and 19h for the stairwell shaft. Overall, the slower vertical transport under $\Delta T \sim 0$ increases the time needed for concentration profiles to stabilize (Figure 8 vs. Figure 6). For the leeward apartment A, comparison between the obtained concentrations to those calculated using the steady-state simulation mode (not shown) indicates that at the 1st and 13th – 15th floors, where concentrations are higher, CO does not reach steady state concentration even after 48h. At elevator shaft, the maximal steady concentration value (C/Cs = 1) was received for all floors only after about 20h. At the stairwell shaft, the concentration profile shows a continuous decrease with floor height (starting from maximal value of 1 at the 1st and 2nd floors), suggesting limited vertical mixing. This latter conclusion is supported by the finding that concentrations at the top floors did not reach steady-state concentration even after 48h. The results were obtained under the assumption that elevator carriage is static. Under conditions associated with movement of elevator carriage pollutant concentration could be pulled higher into the corridor due to the piston effect (Klote 1988).

Results of building temporal response to pollutant transport show that lag-time and build-up rate of pollutant concentration depends on section location and ΔT. Nevertheless, for both ΔT's (reflecting moderate Mediterranean weather) the time needed to reach steady state, even under constant environmental conditions, can be quite long and in many cases may exceed the time of interest for exposure studies (e.g., 8h). Hence, in cases when the time scale of interest is relatively short or under varying meteorological conditions, transient simulation mode is likely to be more reliable.

3.2 Varying weather condition

3.2.1 The effect of meteorological data temporal resolution

Most previous studies simulating indoor transport and resulting concentrations of air pollutants were conducted under the assumption of constant weather conditions. The applicability of such assumption is questionable considering that the time required to reach steady state in multi-story building can be quite long (see previous section), and that over such time intervals outdoor meteorological conditions may vary dramatically. This is especially true in coastal and Mediterranean climate regions that depict a daily meteorological cycle in wind speed and direction due to sea/land breeze. In the following section, the effect of temporal resolution (TR) of input meteorological data (MD) on calculated indoor concentrations and NPL position is tested. The input MD used is based on real-data measured at a Tel-Aviv coastal meteorological station during 15–18

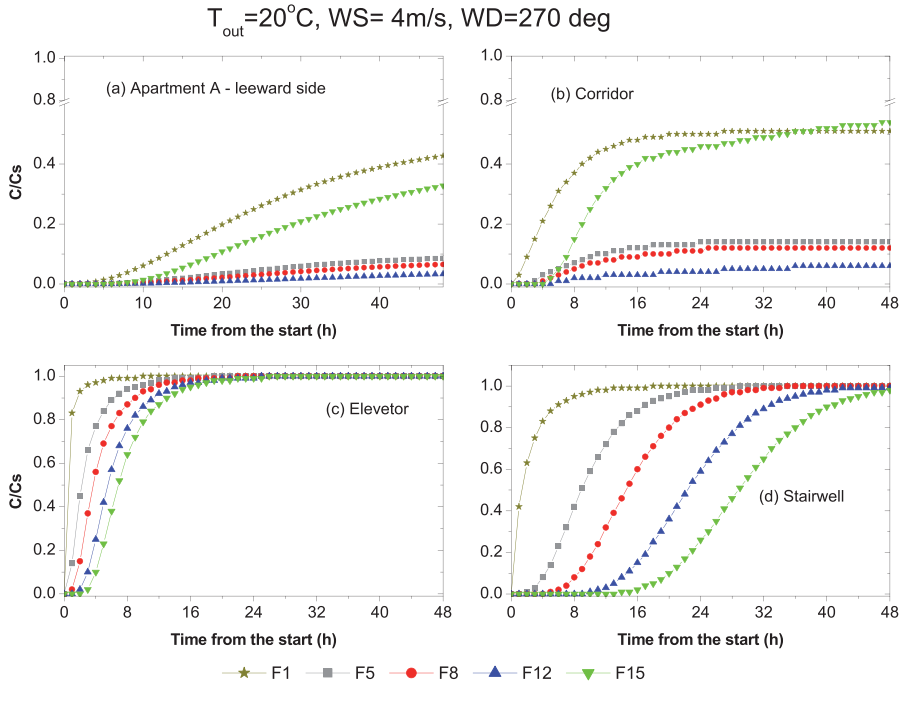

Fig. 8 Variation of normalized concentration over time at selected floors for (a) apartment A, (b) corridor, (c) elevator shaft, and (d) stairwell shaft. Weather conditions: T_{out} = 20 °C, WS = 4 m/s and WD = 270°

January 2017 (IMS Israel Meteorological Service 2020), including 1-hour averaged wind data (direction and speed) and air temperature (Figure 9). For comparison, the same input-data are divided to 8 hours (8h) averaging periods representing morning, afternoon and nighttime hours: 7:00–14:00, 15:00–22:00 and 23:00–6:00. The 8-hour interval is chosen since it is often used for regulation and exposure assessment purposes. Increasing TR below 1 hour will not yield much difference considering that response time of most building sections, regarding pollutant buildup, was found to be longer than an hour. Furthermore, most meteorological stations often provide MD at TR of about 1h. Figures 10 and 11 depict concentration profiles for all four apartments after 8h emission, calculated using 1h and 8h averaged MD (1h-MD and 8h-MD, respectively) as input, during daytime (8:00–16:00) and nighttime hours (22:00–6:00), respectively. Overall, it seems that the effect of the MD-TR on calculated concentration depends primarily on the position of the apartments relative to WD, and to a less extent also on WS and T_{out}. In both tested cases the difference between air concentrations calculated using 1h- and 8h-MD became clear only above the NPL, especially in the uppermost floors (14–15, Figure 10).

The TR effect is larger during daytime hours than at nighttime. During the latter, C/Cs values obtained based on 1h-MD are higher than those obtained with 8h-MD by about 10% to 30% in the windward apartments (A and D; southeast wind), while no difference is observed in the leeward apartments. During the daytime, when temperature and WS are higher, the differences in windward apartments (A and B, northern wind) increase to > 50% and up to a factor of almost 4 (A, 14th floor), while in the leeward apartments (C and D) it is enlarged to 10%–30%. Worth noting that during daytime and nighttime, the concentrations obtained based on 1h-MD are higher than based on 8h-MD in the leeward apartments. In the windward apartments during daytime the opposite trend is observed at all floors above 8h-MD NPL, i.e., C/Cs (8h) > C/Cs (1h).

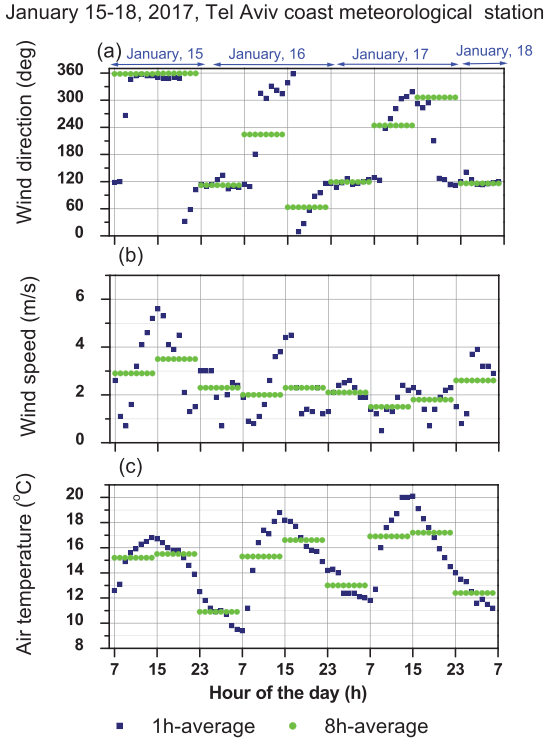

Fig. 9 1h and 8h averages of wind speed, wind direction and temperature measured at Tel-Aviv cost meteorological station on January 15–17, 2017

The effect MD TR on calculated CO concentrations depends strongly on the calculated position of NPL, which is primarily affected by apartment position relative to WD. Under conditions where a similar NPL position is calculated under both TRs (i.e., apartments C and D during day-time, Figure 10), higher concentrations are expected for higher T_{air} and WS values. Accordingly, for the day-time case higher concentrations were received for 1h-MD due to higher calculated T_{air} and WS values (i.e., 16.4 °C and 5.3 m/s for 1h-MD at the 8th hour vs.16.1 °C and 3.8 m/s for 8h-MD). Under conditions where NPL position is affected (i.e., apartments A and B during daytime, Figure 10) higher concentrations will be observed for the MD-TR that yields higher NPL elevation since no pollutant is exiting the shafts below NPL yielding higher pollutant load transfer to upper floors. Indeed, the highest MD-TR effect is observed for apartment B during daytime, where NPL location calculated with 8h-MD is at the 14th floor compared to at the 9th floor for 1h-MD, and simulated [CO] was much higher with 8h-MD than 1h-MD concentrations. In general, the sensitivity to the MD-TR is expected to be lower under more stable meteorological conditions as well as under conditions of stronger stack effect (i.e., larger positive ΔT).

3.2.2 Implementation for human exposure risk assessment

Risk assessment estimation considers the cumulative human exposure to the pollutant over time. Here, exposure estimations are done for the overall tested time interval of 48h. As inhalation exposure is proportional to the air concentration, Figure 12 shows the ratio between averaged concentration calculated using 8h- and 1h-MD (i.e., $\frac{\overline{C(8h)}}{\overline{C(1h)}} = \frac{\Sigma C(8h)}{\Sigma C(1h)}$) in apartments A–D at several selected floors over 72h (MD used as input are presented in Figure 9).

The effect of MD-TR on the accumulated exposure depends primarily on the time that had passed since the beginning of the exposure, as well as on apartment position relative to WD and floor elevation. The strongest effect is observed during the first 28 h for apartments A and B,

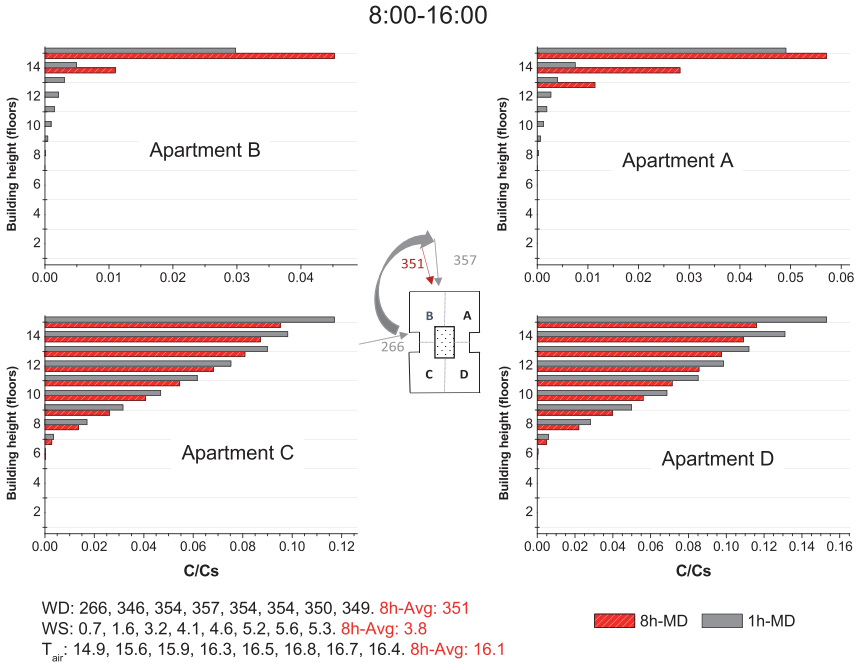

Fig. 10 Vertical profiles of relative concentration after 8h emission, calculated using 1h-MD and 8h-MD as input, for apartments A–D during daytime (8:00–16:00)

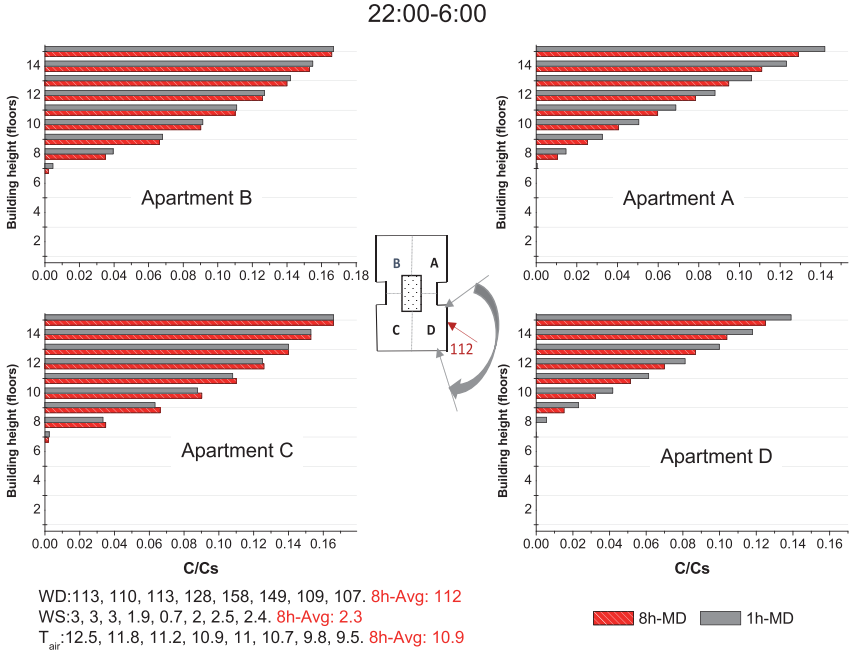

Fig. 11 Vertical profiles of relative concentration after 8h emission, calculated using 1h_MD and 8h-MD as input, for apartments A–D during nighttime (22:00–6:00)

which are on the windward side during day hours when wind is the strongest. During this period, simulation using 8h-MD overestimates concentrations at all floors above 8h-MD NPL (i.e., F12–F15, Figure 12) and underestimates them at floors below 8h-MD NPL and above 1h-MD NPL (i.e., F10, Figure 12). Since in the leeward side both 8h-MD and 1h-MD NPLs are at the same location (apartments C and D, Figure 10), all the presented floors are above NPL, however the extent of the effect is much smaller. While the strongest effect in the windward side is observed as a peak at the 14th floor, in the leeward side it is observed in the closest floor to NPL (F10 for apartments C and D, Figure 12) with a decreasing trend towards higher elevation floors. Over the last 10 h of the simulation the TR effect became minor in

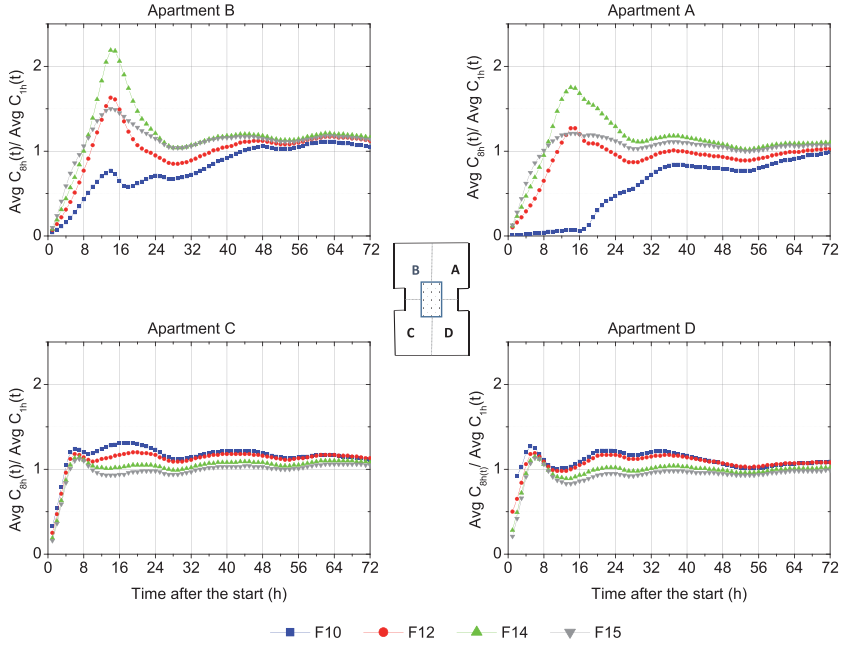

Fig.12 The ratio of the average concentration calculated using 8h-MD (Avg C_{8h} (t)) to the average concentration calculated using 1h-MD (Avg C_{1h} (t)) for apartments A–D in four selected floors over 48 hours. Emission event is set to start at 07:00

all apartments (i.e., calculated air concentrations ratio ~1, Figure 12). The underestimation of indoor concentration calculated using 8h-MD during the first 8h, for all apartments, is an artifact caused by the longer lag time in concentrations buildup above the NPL when using lower TR for MD data input (see also Figure 6). Extending the averaging interval to 12h-MD, generally produced a behavior similar to that obtained with 8h-MD except for the first 12h in the windward apartments (i.e., apartments A and B) where concentration build-up was much lower (data not shown for figure clarity). These results further show that TR of input MD should fit the time scale of interest regarding indoor concentrations. Hence, using daily average MD would be useful for examining long term behavior (i.e., month, season).

Overall, the results presented in the current section indicate that using 8h-MD for assessing human exposure over period of 24h or less might produce inaccurate results. Clearly, the extent of this inaccuracy depends on the variability in the meteorological parameters over this period as well as on WS, ΔT, and position of the apartment of interest (height and direction toward WD).

4 Conclusions

The present study depicts CONTAM simulations of intra-building transport and resulting concentrations of an inert pollutant continuously emitted from an underground garage of a 15-floor building under moderate Mediterranean weather. Wind pressure coefficients are calculated using CFD methods. The study tests two major issues: (1) the temporal response of pollutant build-up at various indoor zones to ambient conditions (air temperature, wind speed and direction) under constant conditions, and (2) the importance of using actual transient meteorological data and the effect of its temporal resolution on simulated indoor air concentrations and resulting exposure. The obtained results indicate the following main points:

- The shape of the vertical profile of AER and CO concentration is sensitive to ΔT, which controls the extent of the stack effect and its importance relative to the wind effect. When both effects dominate ($\Delta T > 0$ and WS > 0), clear NPL is observed and its location depends on WS and the position of facade relative to WD. Under $\Delta T \sim 0$, the NPL is lacking and CO profiles are determined by the WPC profile, yielding null concentrations in the windward side and parabolic-shape profile in the leeward facade (i.e., highest values in top and bottom floors).
- For both ΔT's tested, reflecting moderate Mediterranean weather, the time needed for indoor concentrations to reach steady state, even under constant environmental conditions, was quite long and exceeded common time of interest for exposure studies and regulation (i.e., 8h). Hence, in cases where the timescale of interest is shorter or under varying meteorological conditions, transient simulation mode is likely to be more reliable. It should be noted though that response time of certain sections may be somewhat faster than presented here, if also considering movement of elevator carriages as well as opening of windows and doors. The effect of temporal resolution of MD-input on the accumulated exposure

depends primarily on the time that has passed since the beginning of the exposure, as well as on apartment position relative to WD and floor elevation. Using 8h-averaged MD for assessing human exposure over a period of 24h or less might produce inaccurate results. Clearly, the extent of this inaccuracy depends on the variability in the meteorological parameters over this period as well as on WS, ΔT, and the position of the apartment of interest (height and direction toward WD). Overall, TR of MD used in simulations should fit the time-scale of interest regarding indoor pollutant concentration as well as the response time of pollutant transport in building (i.e., increasing MD-TR beyond the response time will not yield any addition benefit).

The present paper demonstrates the importance of using transient mode simulation and actual meteorological conditions to better estimate indoor concentrations and resulting exposure levels, especially for regulation purposes where timescales of interest are often on the order of a few hours. The temporal resolution of MD-input becomes even more important when considering emission sources that are not constant in time, as often is the case in the indoor environment, as well in buildings located in coastal region where wind conditions change dramatically over a daily cycle due to sea-land breeze.

References

Achakji GY, Tamura GT (1988). Pressure drop characteristics of typical stairshafts in high-rise buildings. *ASHRAE Transactions*, 94: 1223–1237.

ASHRAE (2013). ASHRAE Handbook: Fundamentals. Atalanta: American Society of Heating, Refrigerating and Air-Conditioning Engineers.

Dols W, Polidoro BJ (2015). CONTAM User Guide and Program Documentation Version 3.2.

Eshack A, Leo SDG, Shiva NSM, et al. (2015). Monitoring and simulation of mechanically ventilated underground car parks. *Journal of Thermal Engineering*, 1: 295–302.

Fluent (2013). ANSYS Fluent Theory Guide 15.0. Canonsburg, PA, USA: ANSYS Inc.

IMS Israel Meteorological Service (2020). Goverment portal. Available at https://ims.gov.il/.

ISI (2017). SI 5282 Part 1—Eenergy Rating of Buildings: Residential Buildings. Israel Standard Institute.

Jo J-H, Lim J-H, Song S-Y, et al. (2007). Characteristics of pressure distribution and solution to the problems caused by stack effect in high-rise residential buildings. *Building and Environment*, 42: 263–277.

Klepeis NE, Nelson W, Ott W, et al. (2001). The National Human Activity Pattern Survey (NHAPS): a resource for assessing exposure to environmental pollutants. *Journal of Exposure Analysis and Environmental Epidemiology*, 11: 231–252.

Klote JH (1988). An analysis of the influence of piston effect on elevator smoke control. Gaithersburg, MD, USA: National Bureau of Standards.

Li Y, Duan S, Yu ITS, et al. (2005). Multi-zone modeling of probable SARS virus transmission by airflow between flats in Block E, Amoy Gardens. *Indoor Air,* 15: 96–111.

Liang W, Qin M (2017). A simulation study of ventilation and indoor gaseous pollutant transport under different window/door opening behaviors. *Building Simulation*, 10: 395–405.

Lim T, Cho J, Kim BS (2010). The predictions of infection risk of indoor airborne transmission of diseases in high-rise hospitals: Tracer gas simulation. *Energy and Buildings*, 42: 1172–1181.

Lim T, Cho J, Kim BS (2011). Predictions and measurements of the stack effect on indoor airborne virus transmission in a high-rise hospital building. *Building and Environment*, 46: 2413–2424.

Mao J, Gao N (2015). The airborne transmission of infection between flats in high-rise residential buildings: a review. *Building and Environment*, 94: 516–531.

Mao J, Yang W, Gao N (2015). The transport of gaseous pollutants due to stack and wind effect in high-rise residential buildings. *Building and Environment*, 94: 543–557.

Mu D, Gao N, Zhu T (2016). Wind tunnel tests of inter-flat pollutant transmission characteristics in a rectangular multi-storey residential building, part A: Effect of wind direction. *Building and Environment*, 108: 159–170.

Mu D, Shu C, Gao N, et al. (2017). Wind tunnel tests of inter-flat pollutant transmission characteristics in a rectangular multi-storey residential building, part B: Effect of source location. *Building and Environment*, 114: 281–292.

Papakonstantinou K, Chaloulakou A, Duci A, et al. (2003). Air quality in an underground garage: computational and experimental investigation of ventilation effectiveness. *Energy and Buildings*, 35: 933–940.

Robinson J, Nelson WC (1995). National Human Activity Pattern Survey Data Base. Research Triangle Park, NC, USA: Environmental Protection Agency.

Song D, Yoon S, Jeong C, et al. (2019). Heat, vapor, and CO_2 transportation caused by airflow in high-rise residential buildings. *Building and Environment*, 160: 106176.

Sundell J (2004). On the history of indoor air quality and health. *Indoor Air*, 14: 51–58.

Tominaga Y, Mochida A, Yoshie R, et al. (2008). AIJ guidelines for practical applications of CFD to pedestrian wind environment around buildings. *Journal of Wind Engineering and Industrial Aerodynamics*, 96: 1749–1761.

UNFPA (2007). State of World Population 2007: Unleashing the Potential of Urban Growth. New York: United Nations Population Fund.

Walton GN (1989). AIRNET: A computer program for building airflow network modeling. Gaithersburg, MD, USA: National Institute of Standards and Technology.

Wu Y, Tung TCW, Niu J (2016). On-site measurement of tracer gas transmission between horizontal adjacent Flats in residential building and cross-infection risk assessment. *Building and Environment*, 99: 13–21.

Yang W, Gao N (2015). The transport of gaseous pollutants due to stack effect in high-rise residential buildings. *International Journal of Ventilation*, 14: 191–208.